Research Square

Preprints are preliminary reports that have not undergone peer review.
They should not be considered conclusive, used to inform clinical practice,
or referenced by the media as validated information.

Multi-Objective Optimization of FDM Printing Parameters for Enhanced Tensile Performance of Carbon Fiber-Reinforced PLA Composites

saleh sobhy

salehgaballa@hotmail.com

Higher Technological Institute

Shaimaa M. Mohamed

Modern University For Technology and Information

Asmaa M. Kassab

: 3M Korea

Research Article

Keywords: 3D printing, Tensile strength, Taguchi method, Composite materials, Grey relational analysis, fused deposition modelling

Posted Date: November 6th, 2026

DOI: https://doi.org/10.21203/rs.3.rs-11036357/v1

License: This work is licensed under a Creative Commons Attribution 4.0 International License.
Read Full License

Multi-Objective Optimization of FDM Printing Parameters for Enhanced Tensile Performance of Carbon Fiber-Reinforced PLA Composites

Saleh S. Abdelhady[1, *], Shaimaa M. Mohamed[2] and Asmaa M. Kassab[3]

[1]*Department of Mechanical Engineering, Higher Technological Institute, 10th of Ramadan City, Egypt, P.O. Box: 228*

[2]*Department of Mechanical Engineering, Modern University for Technology and Information, Elmokatam City, Egypt*

[3]*Department of Railway, Egyptian Korean Faculty of industry and energy technology., Beni-Suef Technological University (BTU), Egypt*

* Corresponding author; Email: salehgaballa@hotmail.com (Saleh S. Abdelhady)
Tel: +201028889156; Fax: +20554369819

Abstract

The present work attempts to determine the optimal printing conditions for enhancing tensile performance and investigates the effects of fused deposition modeling (FDM) process parameters on the tensile performance of carbon-fiber-reinforced polylactic acid (PLA-CF) composites. The influence of FDM process parameters, including layer thickness, infill ratio, raster orientation, and printing temperature, was examined using a Taguchi L9 orthogonal array design. To maximize the effect of the process on the tensile characteristics of the 3D printing composite, such as tensile strength, modulus of elasticity, and tensile toughness, a combination of the Taguchi approach and Gray Relational Analysis (GRA) was used. A layer thickness of 0.20 mm, 100% infill, 0° raster orientation, and a printing temperature of 215 °C are the optimal parameters provided by both methods are the same. The optimal values for tensile strength, modulus of elasticity, and tensile toughness, respectively, were found to be 45.2 MPa, 606.943 MPa, and 175.037 MJ/m³, respectively. ANOVA revealed that infill ratio was the most influential parameter, contributing 48.68% to the overall grey relational grade, followed by layer thickness (28.81%), raster orientation (12.02%), and printing temperature (10.50%). These findings highlight the potential of PLA-CF composites for advanced structural and functional component additive manufacturing technologies as well as high-strength engineering applications.

Keywords: 3D printing; Tensile strength; Taguchi method; Composite materials; Grey relational analysis; fused deposition modelling

1.Introduction

One of the most innovative manufacturing technologies in modern engineering is 3D printing, also known as additive manufacturing (AM), which enables the direct fabrication of complex structures from digital models through a layer-by-layer material deposition process [1]. In contrast to traditional subtractive manufacturing methods, additive manufacturing improves production flexibility and customization capabilities while drastically reducing material waste and tooling requirements [2]. The aerospace, automotive, biomedical, electronics, architecture, and defense industries have all seen an increase in the use of additive manufacturing technologies due to their rapid development [3]. Additive manufacturing's significance in industrial and research applications has increased due to its capacity to create lightweight and geometrically complex structures [4].

Fused deposition modeling (FDM) is one of the most popular additive manufacturing techniques due to its low cost, ease of use, and compatibility with thermoplastic materials [5]. FDM technology evolved initially for applications involving rapid prototyping, but it has since developed into a practical manufacturing method for functional engineering components [6]. A thermoplastic filament is heated above its melting point and extruded onto a build platform using a nozzle in accordance with a computer-aided design (CAD) model during the FDM process [7]. After extrusion, the deposited material solidifies, creating successive layers that determine the final component geometry [8]. Layer thickness, nozzle temperature, infill density, raster angle, raster width, print orientation, and printing speed are important FDM processing parameters that have a significant impact on the mechanical performance, surface quality, and dimensional accuracy of printed structures [9].

The mechanical behavior of printed thermoplastic components has been extensively studied because of the growing industrial adoption of FDM [10]. Printed parts frequently have anisotropic characteristics and process-induced flaws that lower structural performance, despite the benefits of FDM in terms of quick fabrication and design flexibility [11]. FDM-fabricated components continue to be severely limited by weak interlayer bonding, residual stresses, void formation, and poor surface finish [12]. The layer-by-layer deposition process, in which the bonding strength between neighboring layers is typically lower than the strength within deposited filaments, is the cause of the anisotropic nature of FDM products [13]. Therefore, building orientation and process parameters affect mechanical characteristics like tensile strength, flexural strength, and impact resistance [14].

Polylactic acid reinforced with carbon fiber (PLA-CF) is one of the most popular composite thermoplastic materials in FDM applications due to its enhanced stiffness, low warping tendency,

ease of processing, and biodegradability [15]. Carbon fiber reinforcements are added to the PLA matrix to create PLA-CF, which improves mechanical and thermal performance for engineering applications [16]. PLA-CF has become very appealing for rapid prototyping and structural manufacturing applications because of its superior printability, lightweight properties, and environmental friendliness [17]. While compared to neat PLA materials, PLA-CF composites show improved dimensional stability, increased stiffness, and decreased thermal shrinkage during printing [18]. Nevertheless, under conditions of high mechanical loading, PLA-CF materials may still display brittleness and interlayer adhesion limitations [19]. Therefore, scientists have investigated various optimization and reinforcement techniques to enhance the mechanical and thermal characteristics of PLA-CF composites made using FDM [20].

Carbon fiber reinforcement is one of the best methods to improve the performance of PLA-CF composites used in additive manufacturing [21]. Carbon fibers are desirable reinforcement materials for thermoplastic composites because of their high tensile strength, superior stiffness, low density, and superior thermal stability [22]. The overall structural rigidity of PLA-CF printed components is improved and stress transfer efficiency is increased by incorporating carbon fibers into PLA matrices [23]. Since carbon fibers are abrasive, they can change the behavior of melt flow and increase nozzle wear [24]. Additionally, in PLA-CF printed specimens, incorrect carbon fiber dispersion and orientation within the PLA matrix may produce stress concentration regions that cause premature mechanical failure [25]. Tensile strength and fatigue resistance of PLA-CF composites can also be decreased by voids and poor interfacial adhesion between the fibers and polymer matrix [26]. Thus, optimizing the performance of PLA-CF printed structures requires careful optimization of printing parameters [27].

Tensile testing is one of the most important mechanical assessments since tensile strength directly represents the load-carrying capacity and structural integrity of printed parts [28]. Process parameters, filament type, thermal history, and internal porosity distribution all influence the tensile behavior of FDM-produced specimens [29]. Changes in printing conditions can impact the initiation and propagation of cracks during mechanical loading by changing the interfacial diffusion between adjacent layers [30]. Thus, to produce mechanically dependable, printed components, FDM process parameter optimization is required [31]. Several investigations have shown that the tensile characteristics of PLA and carbon fiber reinforced composites are greatly impacted by FDM process parameters [32]. In printed specimens, layer thickness has a significant impact on interlayer bonding and porosity formation [33]. Smaller layer thickness values usually increase mechanical strength because they promote better fusion between adjacent layers [34]. Because higher infill percentages minimize internal voids and enhance load transfer throughout the structure, infill density is another significant factor influencing mechanical performance [35].

Additionally, polymer diffusion and molecular entanglement between deposited layers are impacted by nozzle temperature [36].

Among the most important variables influencing anisotropic behavior in FDM-produced parts are raster angle and build orientation [37]. Because stress transfer takes place along continuous filament paths, tensile specimens printed parallel to the loading direction typically show higher tensile strength [38]. Conversely, because of inadequate interlayer bonding strength, perpendicular build orientations frequently result in weaker components [39]. The distribution of stress concentration regions and crack propagation paths during tensile loading are determined by the filament arrangement and raster pattern [40]. For FDM-fabricated components to be more structurally reliable, build orientation optimization is therefore essential [41].

Grey Relational Analysis (GRA) and the Taguchi method are two optimization techniques that are frequently used to find the best set of FDM process parameters for enhancing manufacturing quality and mechanical performance. The Taguchi method is a statistical design of experiments technique that minimizes the number of experimental trials needed while systematically assessing the impact of several process parameters using orthogonal arrays [42]. This technique is highly effective for identifying critical factors affecting tensile strength, surface roughness, dimensional accuracy, and other performance characteristics of FDM-printed components [43]. However, because FDM processes frequently involve multiple performance responses at once, Grey Relational Analysis is frequently integrated with the Taguchi approach to perform multi-objective optimization [44]. The Taguchi method's signal-to-noise (S/N) ratio analysis aids in determining parameter settings that maximize process robustness and minimize variability [45].

The mechanical characteristics of PLA-CF samples made by FDM were examined in this study. The results have primarily been used to assess the tensile strength of PLA-CF material produced under various printing parameters. The test specimens were manufactured using three different parameters: layer thickness, infill ratio, raster orientation, and printing temperature. Additionally, the study yields results that help users choose the best printing and testing parameters for components that are 3D printed. Taguchi-Grey relational analysis was used to optimize process parameters to produce PLA-CF samples. Experiments were conducted at four different levels for an orthogonal layout of L9 with various parameters.

2. Materials and methods

2.1. Filament materials

The thermoplastic filament PLA-CF (1.75 mm diameter, density of 1.22 g/cm3) in this study, produced by bambu lab. Bambu PLA CF is a specially blended tough polylactic acid (PLA) that

has carbon fibers (CF)added to increase its hardness and bending modulus while maintaining the dimensional stability and ease of printing of regular PLA. The mechanical properties of thermoplastic filament PLA-CF are detailed in Tables 1.

Table 1 Mechanical properties of PLA-CF filament.

Tensile Strength (MPa)	Tensile Modulus (MPa)	Breaking elongation (%)
38	2790	8.4

2.2. Procedure parameters

Investigating the relationship between process variables and the tensile characteristics of an additively manufactured part using FDM was the aim of this study. Various specimens were designed to be 3D printed using the FDM technique with various process parameters. These samples were then ready for mechanical testing in the form of uniaxial tension tests which yield a wealth of important information about the behavior of the material under tensile loading. The FDM printer was primarily composed of the extrusion head, working platform, servo device, and filament feedstock. During the FDM process, the filament feedstock was transported into the extrusion head by two feed rolls. The filaments are gradually heated to a semi molten state when the temperature rises above their melting point. The filament feedstock was heated to a semi-molten pattern and extruded from a nozzle with a specified diameter to produce a part with a particular thickness [46]. This study examines the effects of four FDM variable parameters on tensile properties: layer thickness, infill ratio, raster orientation, and printing temperature. The height of the slice that is deposited from the FDM nozzle is known as the layer thickness. The impact of creating thicker or thinner layers on the final quality is investigated using the layer thickness parameter. The quantity of material deposited inside the forms is represented by the infill density. It influences material consumption and establishes the separation between the inner threads. The direction of the material (roads) beads in relation to the part's loading is referred to as the raster angle or orientation. To fill the interior, the deposited roads can be constructed at various angles. Printing temperature establishes the fixed temperature of the nozzle.

2.3. Design of Experiment

The mechanical characteristics of FDM parts are influenced by a variety of factors, including the performance of the molding equipment, the properties of the molding material, processing conditions, post-treatment process measures, and molding process parameters [47,48]. The four process parameters of layer thickness (A), infill ratio (B), raster orientation (C), and printing temperature (D) were examined in the current investigation. Four parameters and three levels of the control variables are presented in Table 2. Tensile specimens have been printed using the

Taguchi method in compliance with the experiment's design for every combination of the L9 orthogonal array design. Nine distinct arranged sets of tests were conducted using the L9 orthogonal array, which was created for four parameters and three levels, as indicated in Table 3. The Taguchi technique evaluates the process variables using a statistical performance metric called the signal-to-noise (S/N) ratio. The S/N ratio is a logarithmic function of the intended output and serves as an optimization objective function [49]. The best quality design and the least variation can be achieved by using the S/N ratio. Increasing the factor weighting effect, reducing mutual action, processing the average and variation simultaneously, and enhancing the quality are all made possible by the S/N ratio. Regardless of the performance characteristic category, a higher S/N ratio corresponds to higher quality characteristics. Each quality characteristic's S/N ratio can be computed independently. The commonly used standard S/N ratios fall into three categories: nominal the best, smaller the better, and larger the better. The S/N ratio in this study is determined using the larger-the-better evaluation, which is defined by:

$$Larger\ the\ better\ S/N\ (db) = -10 * \log_{10}(\frac{1}{n}\sum_{i=1}^{n}\frac{1}{y_i^2}) \quad (1)$$

where n is the number of evaluations and y is the result of those observations of the i^{th} performance characteristic. Furthermore, the percentage contribution of optimized parameters to the responses was evaluated using the statistical technique analysis of variance (ANOVA). Also, the significance of each parameter on the response can be estimated using the results of the ANOVA.

Table 2: Design parameters and their levels

Input parameters	**Symbol**	**Units**	**Levels**		
			1	2	3
Layer thickness	A	mm	0.15	0.2	0.25
Infill ratio	B	%	50	75	100
Raster orientation	C	degree	0	22.5	45
Printing temperature	D	^{O} C	205	215	225

Table 3: The L9 orthogonal array was used for experiments.

Exp. No	**Layer thickness (mm)**		**Infill ratio (%)**		**Raster orientation (°)**		**Printing temperature(^{O} C)**	
	Experimental values	Coded values	Experimental values	Coded values	Experimental values	Coded values	Experimental values	Coded values
1	0.15	1	50	1	0	1	205	1
2	0.15	1	75	2	22.5	2	215	2
3	0.15	1	100	3	45	3	225	3
4	0.2	2	50	1	22.5	2	225	3
5	0.2	2	75	2	45	3	205	1

6	0.2	2	100	3	0	1	215	2
7	0.25	3	50	1	45	3	215	2
8	0.25	3	75	2	0	1	225	3
9	0.25	3	100	3	22.5	2	205	1

2.4. Grey relational analysis (GRA)

To determine the best arrangement of the chosen printing parameters that concurrently maximize tensile strength, modulus of elasticity, and tensile toughness, GRA was used for multi-objective optimization. Using this method, the multiple response procedure's overall evaluation is based on a grey relational grade (GRG). In this case, optimization is achieved by condensing the numerous complex process values into a single GRG. The optimal parametric combination that would yield the highest GRG value is then evaluated. Four steps were involved in the multi-objective optimization process: data normalization, Gray Relational Coefficient (GRC) evaluation, Gray Relational Grade (GRG) computation, and Taguchi analysis of the GRG values[50,51]. The first step involved normalizing the original data, which is a transformation done on a single data input to scale the data into a suitable range and distribute it evenly for additional analysis. The observed values in this study are linearly normalized within the grey relational generating range, which is the range between 0 and 1. The following formula normalizes [0≤$\boldsymbol{X_i}$(**K**)≤ 1], $\boldsymbol{X_i}$(**K**) to reduce variability and avoid the effects of using different units. The larger-is-better approach can be expressed as follows for the quality attributes of the normalized experimental results:

$$\boldsymbol{X_i}(\mathbf{K}) = \frac{\boldsymbol{y_i(k) - min\, y_i(k)}}{\boldsymbol{\max y_i(k) - \min y_i(k)}} \quad (2)$$

The frequency can be stated as, according to the lower-the-better criterion:

$$\boldsymbol{X_i(K)} = \frac{\boldsymbol{max\, y_i(k) - y_i(k)}}{\boldsymbol{max\, y_i(k) - min\, y_i(k)}} \quad (3)$$

Where X_i(K) denotes the value following the formation of the grey connection. The minimum value of $y_i(k)$ for the kth response is min $y_i(k)$, and the maximum value of $\boldsymbol{y_i(k)}$ for the kth response is max $\boldsymbol{y_i(k)}$.

The number of experiments is i = 1, 2, 3, and the number of replies is k = 1, 2, 3. The grey relation coefficient (GRC) is then calculated to ascertain the relationship between the reference sequence and the compatibility sequence. Eq.4 can be used to compute the GRC ($\boldsymbol{\xi}$).

$$\boldsymbol{\xi} = \frac{\boldsymbol{\Delta_{min} + \delta\Delta\, max}}{\boldsymbol{\Delta_i(k) + \delta\Delta max}} \quad (4)$$

Where, $\boldsymbol{\Delta_{oi}\,(k) = \|x_0(k) - x_i(k)\|}$ =difference between absolute value of x0(k) and xi(k); δ is the distinguishing coefficient; 0≤ δ ≤1 To provide replies to equal preference in the present work,

the value of δ was chosen as 0.5[52]. Δ_{min} is the smallest value of Δ_{oi} (k) Δ and $\Delta\, max$ is the largest value of Δ_{oi} (k).

The relevance between two systems or two sequences is measured by the GRG. The GRG is calculated by averaging each performance trait's grey relational coefficient. The total performance characteristic of the multiple response process is determined by the computed GRG. The GRG is described as

$$\gamma_i = \frac{1}{m}\sum_{k=1}^{m} \xi_i(k) \quad (5)$$

Where $\bar{\gamma}_i$ is the mean GRG value is at the desired level for the ith parameter, m is the number of process responses. The ANOVA approach is also used to determine the percentage contribution of each process parameter to the responses and the statistical significance of each component.

2.5 Measurement procedures

In compliance with ASTM D-638 standards, tensile tests were performed on 3D printed specimens of each experiment, with dimensions shown in Fig. (1). Tensile tests with a 10 KN load cell were performed using a universal test machine at a constant speed of 100 mm/min. The tensile toughness of the test samples was also estimated by observing the area under the stress-strain curve in the tensile curves.

The tensile fracture surface morphology of 3D printed specimens were investigated using scanning electron microscope (SEM). Scanning electron microscope (FEI Quanta 250, Hillsboro, Oregon-USA) at the Egypt Desalination Research Center of Excellence (EDRC), [Desert Research Center (DRC), Egypt].

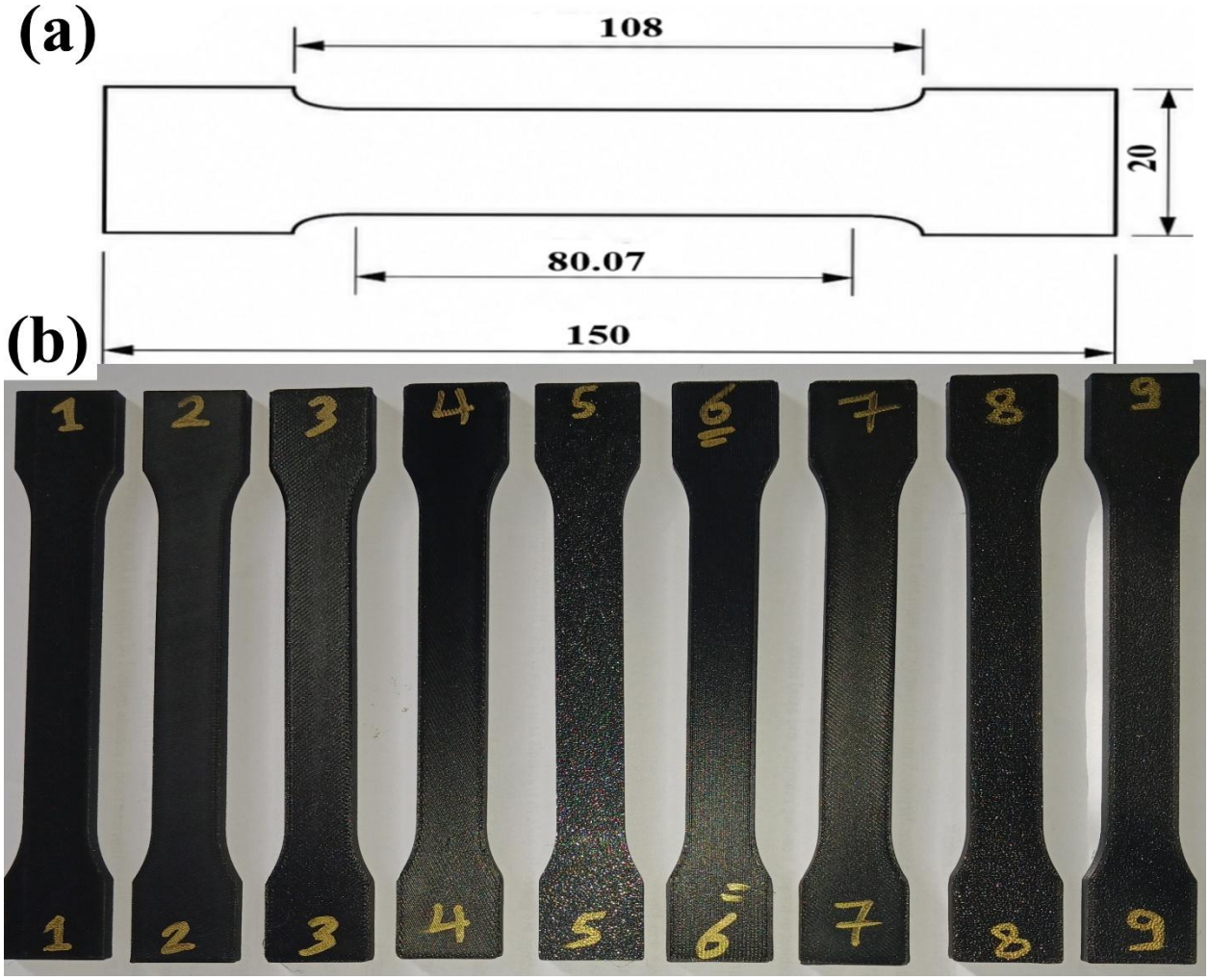


Fig. 1. a) Tensile test specimen, all dimensions are in mm, and b) 3D printed samples

3. Results and discussions

The experimental results converted to S/N ratio values to use the GRA in conjunction with the Taguchi method. This investigation examined the effects of four FDM variable parameters on the ultimate tensile strength, modulus of elasticity, and tensile toughness of 3D printed PLA-CF. The optimum level of each process variable is determined using the signal-to-noise ratio (S/N) approach. According to Taguchi's method, "the larger-the-better analysis" was chosen to examine how the factors affected the responses; in other words, the higher the value, the better the response. The results showed the limitations of first using experimental data for Taguchi method experiments, and the GRA results are described in the second objective.

3.1 Tensile performance and the effect of process parameters

The Taguchi approach was used to determine the S/N ratio and the effect of each printing parameter on the mechanical output of the 3D-printed PLA-CF specimens. This approach's

primary objective is to evaluate quality attributes and reduce deviations from target values to pinpoint the precise factor levels that have a major impact on the process and forecast the best set of variables. The impacts of Layer Thickness (A), Infill Ratio (B), Raster Orientation (C), and Printing Temperature (D) on mechanical properties were thoroughly investigated in this work. The printing parameters are at their ideal levels when the S/N ratio value is larger. Applying such methodical techniques is essential for guaranteeing process stability and improving structural performance, according to research on robust design and parameter optimization in additive manufacturing [53]. The stress-strain curves for the tested 3D-printed specimens are presented in Fig.2. The experimental data for tensile Strength, modulus of elasticity, tensile toughness, and their related S/N ratios were used to identify these trends as shown in Table 4. Each factor's importance was ranked by examining the biggest difference between values (Delta statistics). As shown in Table 5, the factors affecting the ultimate tensile strength are infill ratio, layer thickness, raster orientation, and printing temperature, listed in descending order of significance according to the testing results. Table 6 shows the factors influencing the modulus of elasticity are the infill ratio, layer thickness, raster orientation, and printing temperature, listed in decreasing order of relevance. Lastly, the Tensile Toughness study presented in Table 7 confirms that the infill ratio, layer thickness, raster orientation, and printing temperature are the factors influencing the specimens, listed in the same order of importance.

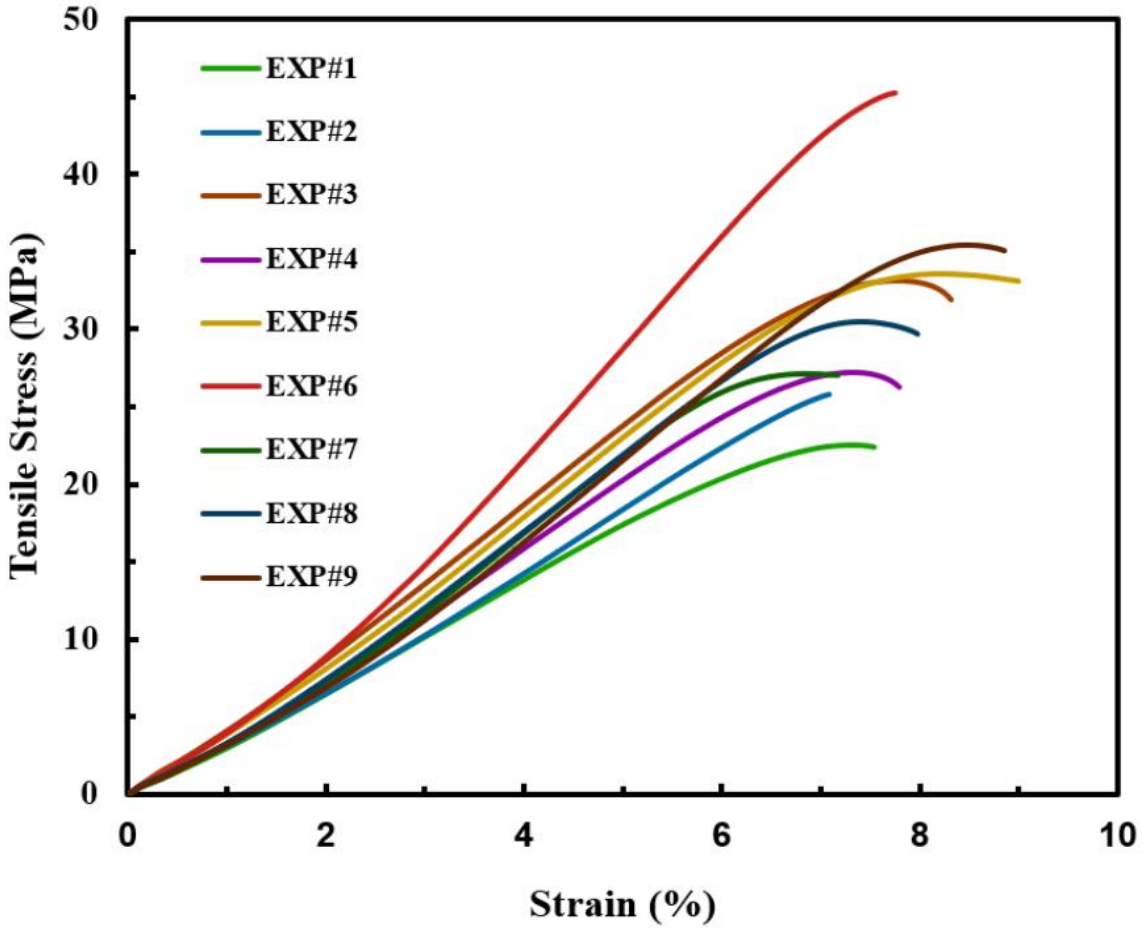


Fig.2.Tensile stress–strain curves for the tested 3D printed samples

Table 4. Experimental results of tensile strength, modulus of elasticity and tensile toughness with their associated S/N ratios based on larger is better

Exp. no.	Tensile strength (MPa)	S/N ratios (dB)	Modulus of Elasticity (MPa)	S/N ratios (dB)	Tensile Toughness (MJ/m^3)	S/N ratios (dB)
1	22.5	27.0437	399.551	52.0314	84.736	38.5614
2	25.8	28.2324	409.587	52.2469	91.848	39.2614
3	33.1	30.3966	475.742	53.5474	137.75	42.7818
4	27.2	28.6914	435.808	52.7859	106.026	40.5082
5	33.6	30.5268	464.843	53.3461	151.032	43.5814
6	45.2	33.1028	606.943	55.663	175.037	44.8626
7	27.1	28.6594	438.73	52.8439	97.153	39.7492
8	30.5	29.686	444.444	52.9563	121.726	41.7076
9	35.4	30.9801	451.689	53.0968	157.286	43.9338

Table 5. Response table for the mean tensile strength and S/N ratios.

Level	Means for Tensile Strength (MPa)				Response for S/N ratios			
	A	B	C	D	A	B	C	D
1	27.13	25.6	32.73	30.5	28.56	28.13	29.94	29.52
2	35.33	29.97	29.47	32.7	30.77	29.48	29.3	30
3	31	37.9	31.27	30.27	29.78	31.49	29.86	29.59
Delta	8.2	12.3	3.27	2.43	2.22	3.36	0.64	0.48
Rank	2	1	3	4	2	1	3	4

Table 6. Response table for the mean modulus of elasticity and S/N ratios.

Level	Means for Modulus of Elasticity (MPa)				Response for S/N ratios			
	A	B	C	D	A	B	C	D
1	428.3	424.7	483.6	438.7	52.61	52.55	53.55	52.82
2	502.5	439.6	432.4	485.1	53.93	52.85	52.71	53.58
3	445	511.5	459.8	452	52.97	54.1	53.25	53.1
Delta	74.2	86.8	51.3	46.4	1.32	1.55	0.84	0.76
Rank	2	1	3	4	2	1	3	4

Table 7. Response table for the mean tensile toughness and S/N ratios.

Level	Means for Tensile Toughness (MJ/m^3)				Response for S/N ratios			
	A	B	C	D	A	B	C	D
1	104.78	95.97	127.17	131.02	40.2	39.61	41.71	42.03
2	144.03	121.54	118.39	121.35	42.98	41.52	41.23	41.29
3	125.39	156.69	128.65	121.83	41.8	43.86	42.04	41.67
Delta	39.25	60.72	10.26	9.67	2.78	4.25	0.8	0.73
Rank	2	1	3	4	2	1	3	4

3.2 Analysis of variance (ANOVA)

ANOVA is used to determine which factor has the greatest influence on the outputs and how input variation affects the outputs. ANOVA approach has been used to evaluate the effect of the printing parameters and identify the crucial factors impacting the mechanical properties of the produced specimens. By analyzing the sum of squares (SS) and percentage contributions, ANOVA is a potent statistical method for quantifying the contribution of each control parameter and identifying the ideal process conditions [54]. The percentage contributions of layer thickness, infill ratio, raster orientation, and printing temperature to the ultimate tensile strength, modulus of elasticity, and tensile toughness are shown in Tables 8, 9, and 10. The contribution percentage reveals each factor's relative ability to lower response variability and highlights its importance in the printing process. A greater impact on the printed components' mechanical performance is correlated with a higher contribution percentage [55].

Table 8. ANOVA table for tensile strength

Symbol	3DPrinting Parameters	DF	Adj SS	Adj MS	Contribution (%)
A	Layer thickness (mm)	2	100.97	50.484	27.96
B	Infill ratio (%)	2	233.3	116.648	64.60
C	Raster orientation (degree)	2	16.06	8.031	4.45
D	Printing temperature (℃)	2	10.82	5.408	3.00
Error		0	—	—	—
Total		8	361.14		100

Table 9. ANOVA table for modulus of elasticity

Symbol	3DPrinting Parameters	DF	Adj SS	Adj MS	Contribution (%)
A	Layer thickness (mm)	2	9104	4552	30.98
B	Infill ratio (%)	2	12910	6455	43.93
C	Raster orientation (degree)	2	3951	1976	13.44
D	Printing temperature (℃)	2	3424	1712	11.65
Error		0	—	—	—
Total		8	29390		100

Table 10. ANOVA table for tensile toughness

Symbol	3DPrinting Parameters	DF	Adj SS	Adj MS	Contribution %
A	Layer thickness (mm)	2	2313.2	1156.6	28.03
B	Infill ratio (%)	2	5576.3	2788.13	67.57
C	Raster orientation (degree)	2	184.5	92.25	2.24
D	Printing temperature (℃)	2	178.1	89.07	2.16
Error		0	—	—	—
Total		8	8252.1		100

Based on data from ANOVA Table 8, the infill ratio is the most important factor affecting the ultimate tensile strength, accounting for 64.60% of the overall variation, while the layer thickness comes in second with a contribution of 27.96%. The raster orientation and printing temperature have comparatively small effects, contributing 4.45% and 3.00%, respectively. Table 9 shows that the modulus of elasticity is most affected by the infill ratio, which contributes 43.93% of the total variation, followed by layer thickness, which contributes 30.98%. The contributions of printing temperature and raster orientation are 13.44% and 11.65%, respectively. Additionally, as Table 10 illustrates, the infill ratio accounts for 67.57% of the total variation in tensile toughness, whereas layer thickness accounts for 28.03%. Raster orientation and printing temperature, on the other hand, had little effects, contributing 2.24% and 2.16%, respectively.

3.3 Development of linear and multiple regression model

The relationship between the printing parameters and the resulting mechanical qualities was mathematically represented by first-order polynomial regression models. The multi-regression analysis of the experimental design matrix and the matching response values for each mechanical characteristic served as the foundation for the development of these equations, which are displayed below:

$$\begin{aligned}\text{Tensile strength (MPa)} = {} & 31.16 - 4.022\ A_1 + 4.178\ A_2 - 0.1556\ A_3 - 5.556\ B_1 \\ & - 1.189\ B_2 + 6.744\ B_3 + 1.578\ C_1 - 1.689\ C_2 + 0.1111\ C_3 \\ & - 0.6556\ D_1 + 1.544\ D_2 - 0.8889\ D_3 \end{aligned} \quad (6)$$

$$\begin{aligned}\text{Modulus of elasticity (MPa)} = {} & 458.6 - 30.30\ A_1 + 43.94\ A_2 - 13.64\ A_3 - 33.90\ B_1 \\ & - 18.97\ B_2 + 52.87\ B_3 + 25.05\ C_1 - 26.23\ C_2 + 1.179\ C_3 \\ & - 19.90\ D_1 + 26.49\ D_2 - 6.595\ D_3 \end{aligned} \quad (7)$$

$$\begin{aligned}\text{Tensile toughness (MJ/m}^3\text{)} = {} & 124.7 - 19.95\ A_1 + 19.30\ A_2 + 0.6557\ A_3 - 28.76\ B_1 \\ & - 3.197\ B_2 + 31.96\ B_3 + 2.434\ C_1 - 6.346\ C_2 \\ & + 3.913\ C_3 + 6.285\ D_1 - 3.386\ D_2 - 2.899\ D_3 \end{aligned} \quad (8)$$

To assess the statistical significance and reliability of the developed regression models for ultimate tensile strength, modulus of elasticity, and tensile toughness, an analysis of variance (ANOVA) was performed. The validity and predictive accuracy of these models, represented by Eqs (6), (7), and (8), are systematically evaluated through the ANOVA results presented in Tables 8, 9, and 10.

3.4 Analyzing the results of experiments

The Taguchi L9 orthogonal array was utilized to investigate the impact of various printing parameters (layer thickness, infill ratio, raster orientation, and printing temperature) on the tensile properties of the 3D-printed PLA-CF composites. Three levels were considered for each parameter: layer thickness (0.15, 0.20, and 0.25 mm), infill ratio (50, 75, and 100%), raster orientation (0°, 22.5°, and 45°), and printing temperature (205, 215, and 225 °C).

The experimental results indicated that the selected process parameters had a significant impact on the tensile strength, modulus of elasticity, and tensile toughness of the printed composites. Tensile strength ranged from 22.5 MPa to 45.2 MPa, and modulus of elasticity varied from 399.551 MPa to 606.943 MPa. Additionally, the tensile toughness displayed a broad range of values, ranging from 84.736 to 175.037. These variations demonstrate how printing circumstances significantly affect the mechanical performance of PLA-CF composites.

Fig.3(a–c) illustrates how the process factors affect the tensile strength, modulus of elasticity, and tensile toughness. The maximum tensile strength (45.2 MPa), modulus of elasticity (606.943

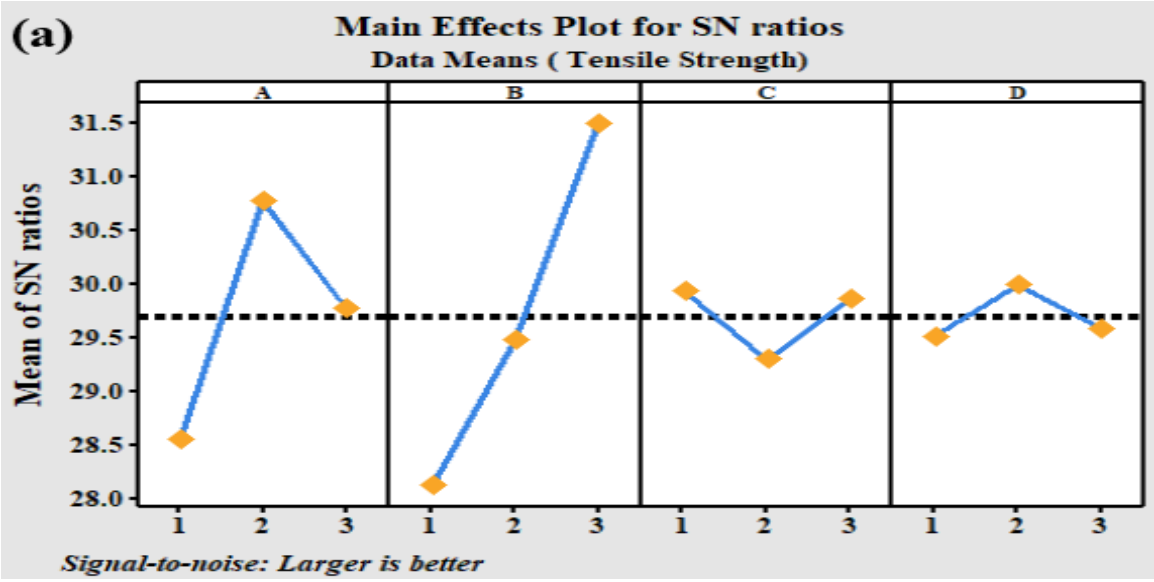
MPa), and tensile toughness (175.037) were found for experiment No. 6, which was constructed with a layer thickness of 0.20 mm, an infill ratio of 100%, a raster orientation of 0°, and a printing temperature of 215 °C.

The combined effect of the infill ratio and raster orientation results in improved mechanical performance under these processing conditions. Increasing the infill ratio reduces internal porosity and increases the effective load-bearing surface, improving the distribution of stress inside the composite structure. Previous studies have demonstrated that specimens printed with high infill percentages have superior mechanical characteristics because of the reduced void content and enhanced interfacial bonding between adjacent filaments [56,57]. Layer thickness has a significant effect on the tensile performance of FDM-printed composites. A moderate layer thickness facilitates better molecular mobility at the interfaces and enhances the fusion between subsequent layers. On the other hand, very thick layers may reduce interlayer adhesion and raise the likelihood of defect formation, while extremely thin layers lengthen the production process [58]. According to the findings, the intermediate layer thickness of 0.20 mm offered the optimal compromise between printing efficiency and structural integrity. Raster orientation has an enormous influence on the anisotropic mechanical response of the printed specimens. When the raster orientation was parallel to the loading direction (0°), the maximum tensile characteristics were obtained, suggesting more effective stress transfer along the deposited filaments. Increasing the raster angle to 22.5° and 45° changed the stress distribution and promoted fracture initiation at the interfaces between adjacent highways, resulting in lower tensile strength and stiffness. Similar results have been found in earlier research on carbon-fiber-reinforced PLA composites created using fused deposition modeling [59,60].

Another crucial factor influencing the bonding quality between adjacent layers is printing temperature. Polymer chain mobility and the diffusion process across layer interfaces are both improved by raising the nozzle temperature. On the other hand, high temperatures can cause the polymer matrix to deteriorate thermally and have a detrimental impact on mechanical performance. The current findings show that the best interlayer adhesion and the maximum tensile characteristics were obtained at a printing temperature of 215 °C [61]. In terms of tensile toughness, experiment No. 6 had the highest value, whereas experiment No. 1 had the lowest value. The enhancement of fiber-matrix interaction and the decrease of internal flaws under ideal printing circumstances can account for this trend. Improved layer consolidation boosts the composite's capacity to absorb energy before failure and slows the spread of cracks [62]. Overall, the experimental findings verify that enhancing the tensile strength, stiffness, and toughness of PLA-CF composites requires fine-tuning the FDM process parameters. Improved interlayer bonding, less porosity, advantageous

fiber orientation, and more effective stress-transfer mechanisms inside the printed structure are the primary causes of the reported improvements.

Based on the suggested regression model, numerical optimization was used to determine the optimal set of process parameters for optimizing the tensile strength, modulus of elasticity, and tensile toughness of the PLA-CF, as seen in Fig. 4. A layer thickness of 0.20 mm, an infill ratio of 100%, a raster orientation of 0°, and a printing temperature of 215 °C were determined to be the optimum parameters. The composite desirability obtained its maximum value under these circumstances, demonstrating a high degree of agreement between the target and predicted responses. The improvement in mechanical properties is due to better interlayer bonding and a reduction in internal defects and voids in the printed structure. Furthermore, the parallel orientation of the deposited filaments to the loading direction improved the composite's ability to support loads and facilitated efficient stress transmission. Additionally, the structural integrity of the printed specimens was enhanced by the full infill density, and the selected printing temperature for enough polymer diffusion between successive layers without causing thermal degradation. Similar results have been documented in earlier research, which showed that by improving fiber–matrix interaction and reducing porosity, regression-based optimization strategies successfully enhance the mechanical performance of carbon-fiber-reinforced PLA composites [63].



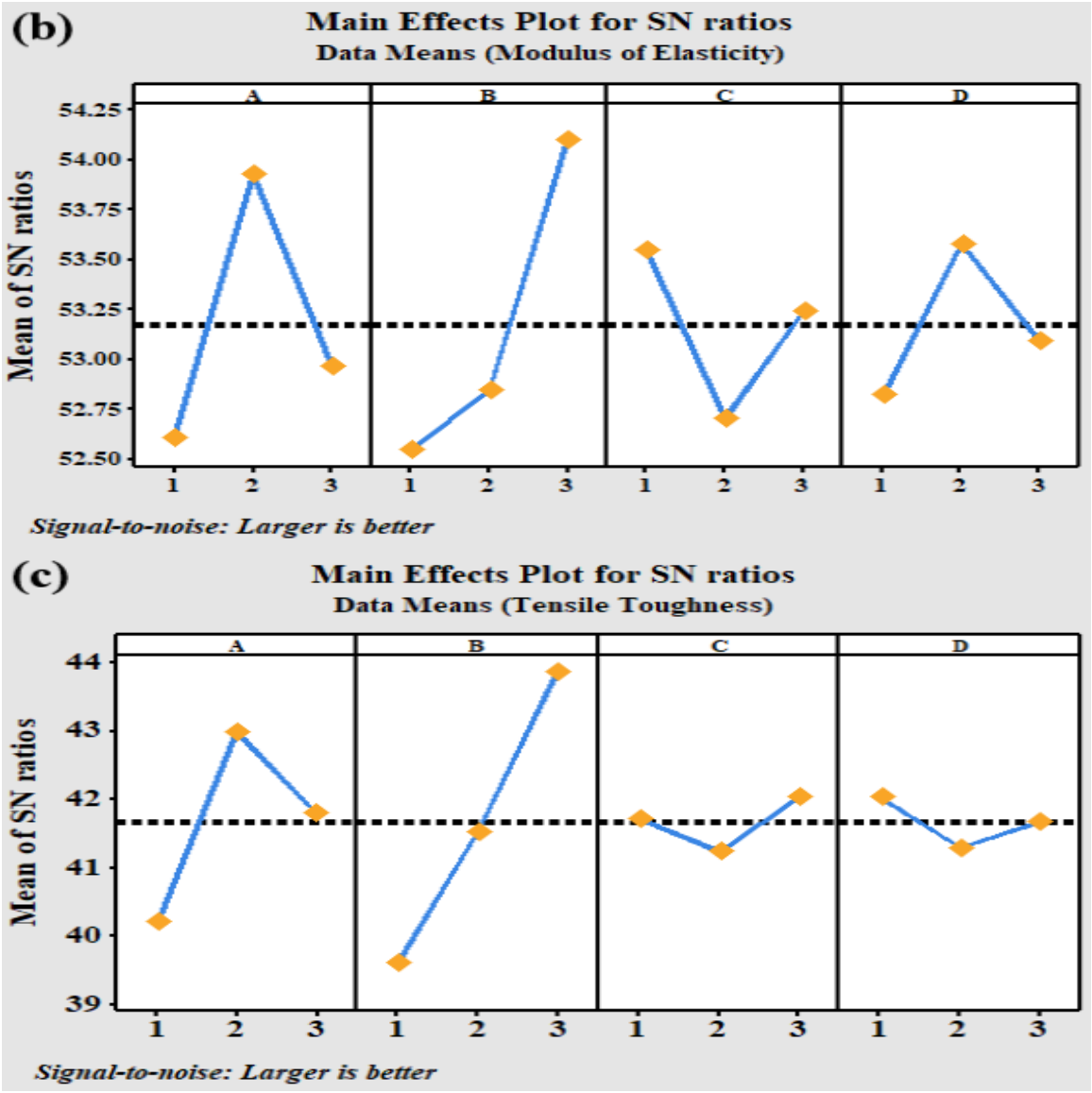


Fig. 3 Response graph for procedure variables effects on tensile strength (a), modulus of elasticity (b), and tensile toughness (c).

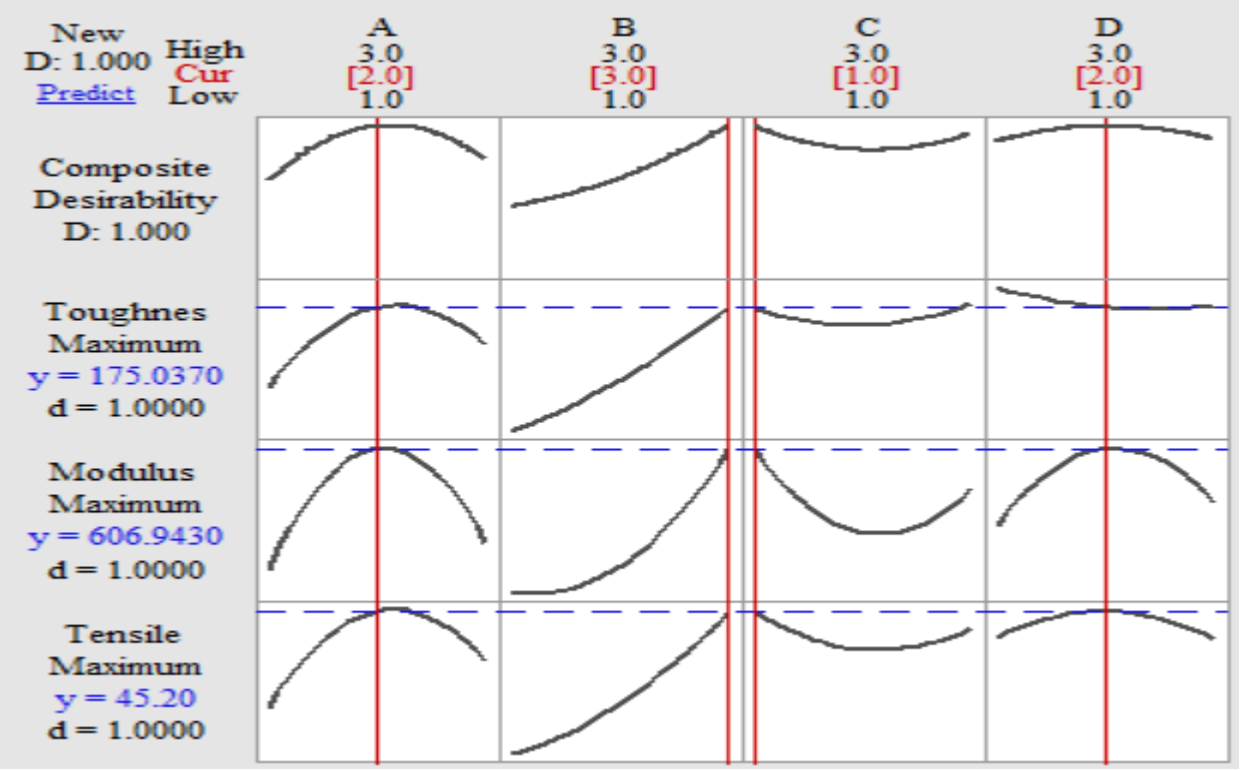


Fig.4 Optimum variables for maximum tensile strength, modulus of elasticity, and tensile toughness

3.5 Taguchi grey relational analysis

Multi-objective optimization problems cannot be optimized using the common Taguchi method. Gray relational analysis (GRA) and the Taguchi approach are used to optimize multi-objective problems to get around this. Multi-objective optimization problems are reduced to single-objective problems using the gray relational analysis method. Next, the optimal set of variables is assessed. This results in the highest gray relational grade (GRG) [64,65]. The signal-to-noise (S/N) ratio is a statistical performance metric that the Taguchi technique uses to evaluate the process variables. The experimental data was first standardized using the "larger-the-better" criterion, and then the deviation sequences and gray relational coefficients were calculated. The multi-response optimization problem was transformed into a single performance indicator, the gray relational grade (GRG), which concurrently included tensile strength, modulus of elasticity, and tensile toughness using gray relational analysis (GRA). The GRA approach normalizes the data (means) into a similar sequence between 0 and 1. Table 11 displays the normalized responses together with the associated deviation coefficients, while Table 12 lists the computed grey relational coefficients, grey relational grades, and signal-to-noise ratios.

The GRG values, which ranged from 0.333 to 1.000, showed that the overall mechanical performance of the printed PLA-CF composites under different printing parameters varied considerably. A combination of 0.20 mm layer thickness, 100% infill ratio, 0° raster orientation,

and 215 °C printing temperature produced the best overall mechanical performance, according to experiment no. 6, which had the highest gray relational grade (GRG = 1.000) among the investigated experiments. In contrast, the lowest GRG value (0.333) was found in experiment no.1. The response table for signal to noise (S/N) ratios and geometric mean (GRG) is presented in table 13. The results show that the optimal printing parameters are A2, B3, C1, and D2, which correspond to a layer thickness of 0.20 mm, an infill ratio of 100%, a raster orientation of 0°, and a printing temperature of 215 °C. Furthermore, these settings were validated by numerical optimization analysis, which proved the reliability of the optimization method. Additionally, the infill ratio had the biggest impact on the grey relational grade, according to the delta values, followed by layer thickness, raster orientation, and printing temperature. This phenomenon is explained by the fact that infill density has a major role in regulating the internal structure, porosity, and load-bearing capacity of composites made of PLA [66].

Table 11. Estimation of normalized data for each response and deviation coefficients.

Exp. No.	Normalized data ($X_i(K)$)			Deviation coefficients(Δio)		
	Tensile strength	Modulus of elasticity	Tensile toughness	Tensile strength	Modulus of elasticity	Tensile toughness
1	0	0	0	1	1	1
2	0.145	0.048	0.078	0.855	0.952	0.922
3	0.467	0.367	0.587	0.533	0.633	0.413
4	0.207	0.175	0.236	0.793	0.825	0.764
5	0.489	0.315	0.734	0.511	0.685	0.266
6	1	1	1	0	0	0
7	0.203	0.285	0.137	0.797	0.715	0.863
8	0.352	0.216	0.410	0.648	0.784	0.590
9	0.568	0.251	0.804	0.432	0.749	0.196

Table 12. Grey relational coefficient, grey relational grade, and S/N ratios.

Exp. No.	Grey relational coefficient (ξi (k))			grey relational grade (ϒi)	S/N ratios (db)
	Tensile strength	Modulus of elasticity	Tensile toughness		
1	0.333	0.333	0.333	0.333	-9.54243
2	0.369	0.344	0.352	0.355	-8.99359
3	0.484	0.441	0.548	0.491	-6.17733
4	0.387	0.377	0.396	0.387	-8.25681
5	0.495	0.422	0.653	0.523	-5.62804
6	1	1	1	1	0.00000
7	0.385	0.412	0.367	0.388	-8.22329
8	0.436	0.390	0.459	0.428	-7.37234
9	0.537	0.400	0.719	0.552	-5.16283

Table 13. The means of GRG and estimated S/N response.

Level	Means of GRG				Response for S/N ratios			
	A	B	C	D	A	B	C	D
1	0.3932	0.3693	0.5871	0.4694	-8.238	-8.674	-5.638	-6.778
2	0.6365	0.4354	0.4312	0.581	-4.628	-7.331	-7.471	-5.739
3	0.4559	0.681	0.4674	0.4352	-6.919	-3.78	-6.676	-7.269
Delta	0.2434	0.3117	0.1559	0.1459	3.609	4.894	1.833	1.53
Rank	2	1	3	4	2	1	3	4

3.6 ANOVA Evaluation for GRG

The results of the ANOVA method used to evaluate the effects of the parameters on GRG and analyze the GRG results are provided in Table 14. Significant procedure variables and the corresponding percentage contributions to the GRG of 3D printing samples have been examined using analysis of variance. The infill ratio was shown to be the most significant factor, accounting for 48.68% of the total performance. Layer thickness, raster orientation, and printing temperature came in second, third, and fourth, respectively, with contribution percentages of 28.81%, 12.02%, and 10.50%.

The predominance of the infill ratio indicates that the mechanical performance of the printed PLA-CF composites is significantly influenced by the internal density and bonding quality between adjacent filaments. Increasing the infill ratio reduces internal voids and increases the effective load-carrying area, which improves the printed specimens' stiffness and strength [67,68]. Following response values (GRG), multiple regression analysis, and ANOVA have been accomplished, establishing the following first-order polynomial equation:

$$GRG = 0.4952 - 0.1021\,A_1 + 0.1413\,A_2 - 0.03927\,A_3 - 0.1259\,B_1 - 0.05984\,B_2 + 0.1858\,B_3 + 0.09188\,C_1 - 0.06405\,C_2 - 0.02782\,C_3 - 0.02577\,D_1 + 0.08581\,D_2 - 0.06005\,D_3 \quad (9)$$

The optimal amounts of the variables under investigation were found using the regression equation that was established. As a result, it offers a useful instrument for assessing how the chosen parameters affect the overall mechanical performance [69].

Table 14. Analysis of Variance for GRG

Symbol	Printing Parameters	DF	Adj SS	Adj MS	Contribution %
A	Layer thickness (mm)	2	0.09579	0.04790	28.81
B	Infill ratio (%)	2	0.16185	0.08093	48.68
C	Raster orientation (degree)	2	0.03995	0.01998	12.02
D	Printing temperature (℃)	2	0.03490	0.01745	10.50
Error		0	—	—	—
Total		8	0.33250		100.00

3.7 The optimal value for each variable

The gray relationship grade variation under various printing conditions is shown in Figure 5. At 0.20 mm layer thickness, 100% infill ratio, 0° raster orientation, and 215 °C printing temperature, the greatest GRG value was achieved. For the best overall mechanical performance, this combination was shown to be the ideal circumstance. Additionally, the Taguchi orthogonal array's usefulness in improving the combined mechanical responses is demonstrated by the fact that the resulting optimum configuration matches one of the experiments.

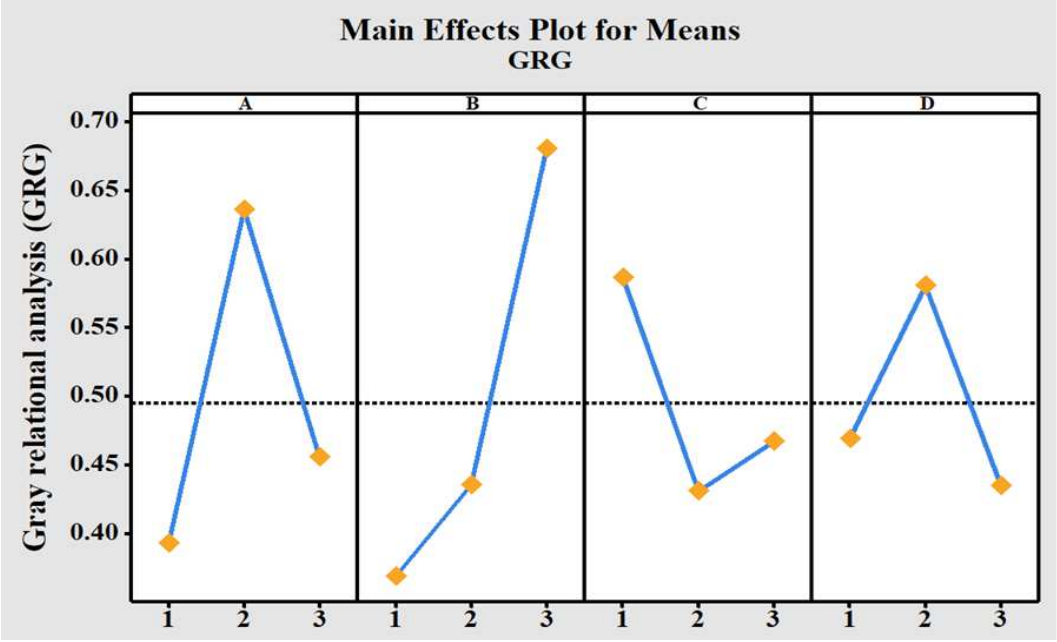


Fig. 5 Response graph for procedure variables effects on GRG

3.8 Microstructure assessment of the tensile fracture surface

SEM micrographs of the fractured surfaces of nine carbon fiber-reinforced polylactic acid (PLA-CF) specimens that were 3D printed and matched the L9 Taguchi experimental design are shown in Figure 6. The fracture morphologies show that filament consolidation, interlayer bonding, void formation, and the overall failure mechanism of the PLA-CF composites are significantly

influenced by printing parameters, such as layer thickness, infill ratio, raster orientation, and printing temperature. The interaction between the short carbon fibers and the PLA matrix also controls the fracture behavior of PLA-CF, in contrast to neat PLA. Prior studies have shown that during fused deposition modeling (FDM), carbon fibers preferentially align along the direction of material deposition, leading to anisotropic mechanical properties and direction-dependent stress transfer [70,71].

The SEM images of Exp.1 and Exp.2 show comparatively uneven fracture surfaces with distinct interfacial gaps and boundaries between neighboring deposited filaments. These flaws show restricted molecular diffusion across the filament interfaces and incomplete fusion between subsequent layers. Under tensile loading, these discontinuities serve as areas of concentrated stress and promote the formation of cracks. Carbon fibers can increase the stiffness of PLA-CF composites, but inadequate thermal bonding or poor fiber–matrix adhesion may encourage fiber pull-out and interfacial debonding during fracture [72]. While there are still distinct boundaries between deposited rasters, Exp. 3, Exp. 4, and Exp. 5 show somewhat better filament consolidation. There are areas of matrix tearing and localized roughness on the fracture surfaces, indicating that interlayer separation and PLA matrix fracture combined to cause crack propagation. Increased energy absorption during fracture is typically linked to the rougher morphology. Specifically, the increased resistance to crack propagation resulting from better consolidation and carbon-fiber-induced crack deflection may be responsible for the higher tensile toughness seen in Exp. 3 and Exp. 5. Because carbon fibers are primarily aligned along the extrusion direction, the orientation of the deposited raster is especially crucial. When the filaments are favorably oriented with respect to the applied tensile load, more effective stress transfer is possible [73].

The fracture morphology was most consistent and compact in experiment no. 6. Despite the presence of triangular defects and localized voids, its SEM micrograph shows a relatively dense and well-consolidated layered structure in comparison to several other experiments. The combination of 0.20 mm layer thickness, 100% infill ratio, 0° raster orientation, and 215°C printing temperature can be linked to Exp.6's superior characteristics. Internal porosity is reduced by the full infill ratio, and improved stiffness and efficient load transfer are promoted by the 0° raster orientation, which more closely aligns the embedded carbon fibers and deposited filaments with the direction of tensile loading. Additionally, a suitable printing temperature enhances interfacial diffusion and polymer flow without causing the PLA matrix to deteriorate too much [74].

The fracture surfaces of Exp.7, Exp.8, and Exp.9 show more pronounced filament interfaces and localized interlayer separation. These short-fiber-reinforced thermoplastic composites are expected to fail due to carbon fiber pull-out, matrix cracking, and debonding at the fiber–matrix interface. The efficiency of stress transfer can be decreased and localized crack propagation can

be started by the presence of voids where fibers were previously embedded. However, compared to Exp.7 and Exp.8, Exp.9 shows comparatively better mechanical performance, suggesting that the combined printing conditions enhanced structural consolidation. Tensile performance and fracture morphology are strongly correlated, according to the SEM observations. Superior strength, stiffness, and toughness were achieved through dense filament packing, decreased porosity, enhanced interlayer adhesion, and advantageous carbon fiber alignment. On the other hand, fiber-matrix debonding, large interlayer gaps, and inadequate consolidation encouraged early failure. These results demonstrate that improving the mechanical performance of PLA-CF components and minimizing the intrinsic anisotropy related to layer-by-layer additive manufacturing depend on FDM parameter optimization [75].

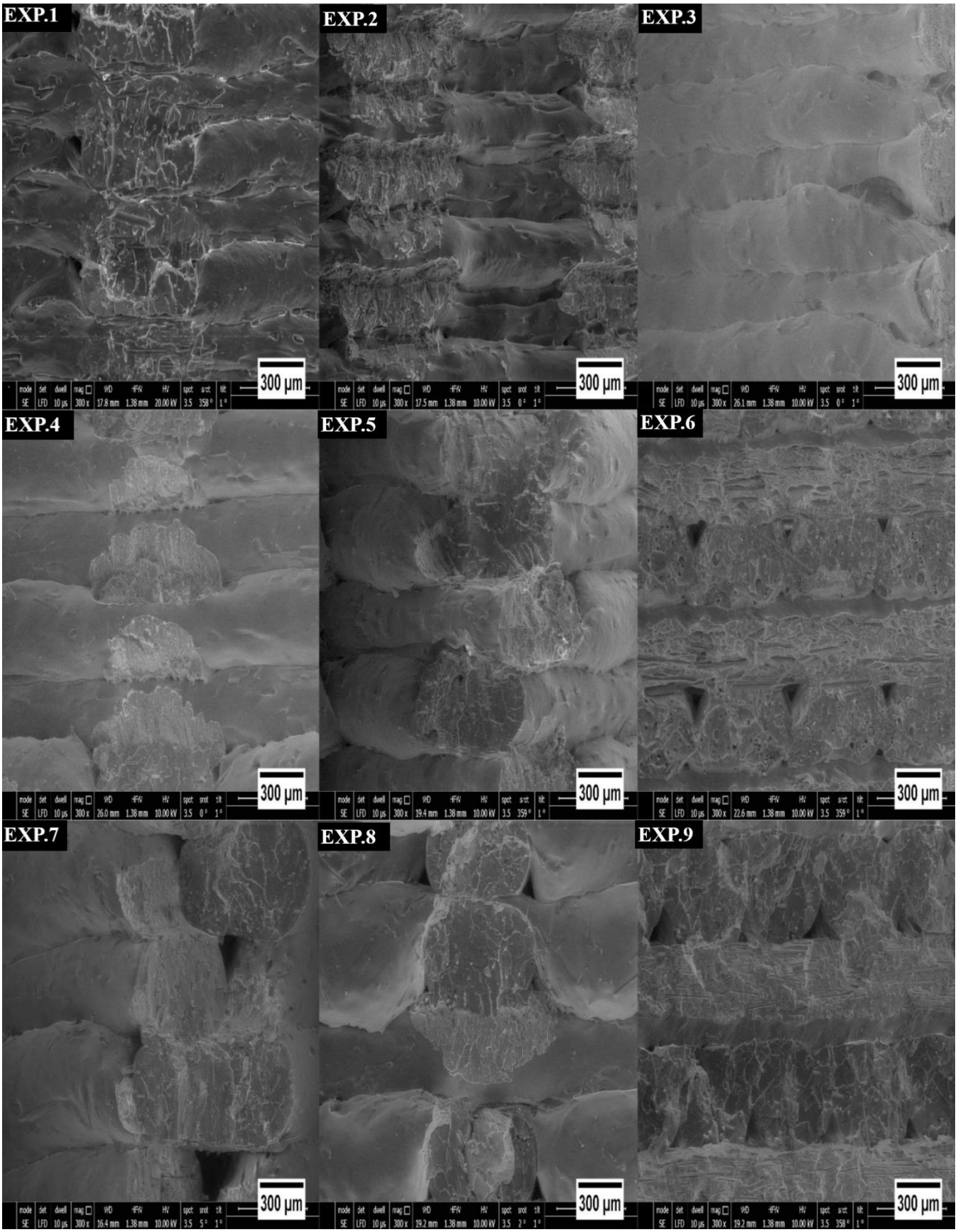


Fig. 6: Fracture surface of the tensile sample

4.Conclusion

The current study investigated the effects of FDM processing parameters on the mechanical performance of 3D-printed PLA-CF composites using a Taguchi L9 experimental design and Gray Relational Analysis. Three levels of investigation were conducted for four significant process variables: layer thickness, infill ratio, raster orientation, and printing temperature. The primary performance responses were determined to be tensile strength, modulus of elasticity, and tensile toughness. The study came to the following conclusions:

1- The results revealed how the Taguchi technique and GRA could be used to determine the optimal FDM processing parameters for fabricating a PLA-CF composite.

2- ANOVA of the grey relational grade further demonstrated that infill ratio was the dominant parameter, with a contribution of 48.68%, followed by layer thickness (28.81%), raster orientation (12.02%), and printing temperature (10.50%).

3- The results have the largest gray relational grade of 1, indicating higher tensile strength, modulus of elasticity, and tensile toughness.

4- The optimum condition within the examined parameter range is represented by the combination of 0.20 mm layer thickness, 100% infill, 0° raster orientation, and 215 °C printing temperature.

5- The predicted optimal FDM processing parameters yielded maximum values of 45.2 MPa for tensile strength, 606.943 MPa for modulus of elasticity, and 175.037 MJ/m^3 for tensile toughness.

6- The results of this study are advantageous for applications of polymeric mechanical metamaterials with high strength.

Acknowledgments:

No funding sources that supported the research were presented.

Author contributions:

All authors have read and agreed with the research presented.

Conflict of interest:

The authors declare that there is no conflict of interest.

Data and code availability: Not applicable

Supplementary Information: Not applicable

Ethical approval: Not applicable

References

1. Gibson, I., Rosen, D. W., & Stucker, B. (2021). Additive manufacturing technologies: 3D printing, rapid prototyping, and direct digital manufacturing (3rd ed.). Springer.
2. Ngo, T. D., Kashani, A., Imbalzano, G., Nguyen, K. T., & Hui, D. (2018). Additive manufacturing (3D printing): A review of materials, methods, applications and challenges. Composites Part B: Engineering, 143, 172–196.
3. Javaid, M., & Haleem, A. (2019). Additive manufacturing applications in medical cases: A literature-based review. Alexandria Journal of Medicine, 54(4), 411–422.
4. Kumar, L. J., Nair, C. K., Jayakumar, A., & Mathew, A. (2021). Additive manufacturing in aerospace and automotive industries. Materials Today: Proceedings, 45, 4893–4898.
5. Turner, B. N., Strong, R., & Gold, S. A. (2014). A review of melt extrusion additive manufacturing processes: I. Process design and modeling. Rapid Prototyping Journal, 20(3), 192–204.
6. Chacón, J. M., Caminero, M. A., García-Plaza, E., & Núñez, P. J. (2017). Additive manufacturing of PLA structures using fused deposition modelling: Effect of process parameters on mechanical properties and their optimal selection. Materials & Design, 124, 143–157.
7. Ahn, S. H., Montero, M., Odell, D., Roundy, S., & Wright, P. K. (2002). Anisotropic material properties of fused deposition modeling ABS. Rapid Prototyping Journal, 8(4), 248–257.
8. Tymrak, B. M., Kreiger, M., & Pearce, J. M. (2014). Mechanical properties of components fabricated with open-source 3-D printers under realistic environmental conditions. Materials & Design, 58, 242–246.
9. Rajpurohit, S. R., & Dave, H. K. (2018). Analysis of tensile strength of a fused filament fabricated PLA part using Taguchi method. Rapid Prototyping Journal, 24(8), 1317–1324.

10. Ziemian, C., Sharma, M., & Ziemian, S. (2012). Anisotropic mechanical properties of ABS parts fabricated by fused deposition modelling. In Mechanical engineering (pp. 159–180). InTech.
11. Bellini, A., & Güçeri, S. (2003). Mechanical characterization of parts fabricated using fused deposition modeling. Rapid Prototyping Journal, 9(4), 252–264.
12. Sun, Q., Rizvi, G. M., Bellehumeur, C. T., & Gu, P. (2008). Effect of processing conditions on the bonding quality of FDM polymer filaments. Rapid Prototyping Journal, 14(2), 72–80.
13. Li, L., Sun, Q., Bellehumeur, C., & Gu, P. (2002). Composite modeling and analysis for fabrication of FDM prototypes with locally controlled properties. Journal of Manufacturing Processes, 4(2), 129–141.
14. Cantrell, J. T., Rohde, S., Damiani, D., Gurnani, R., DiSandro, L., Anton, J., Young, A., Jerez, A., Steinbach, D., Kroese, C., & Ifju, P. (2017). Experimental characterization of the mechanical properties of 3D-printed ABS and polycarbonate parts. Rapid Prototyping Journal, 23(4), 811–824.
15. Drumright, R. E., Gruber, P. R., & Henton, D. E. (2000). Polylactic acid technology. Advanced Materials, 12(23), 1841–1846.
16. Auras, R., Harte, B., & Selke, S. (2004). An overview of polylactides as packaging materials. Macromolecular Bioscience, 4(9), 835–864.
17. Anderson, K. S. (2008). Thermal and mechanical properties of polylactic acid composites. Polymer Engineering & Science, 48(5), 1019–1027.
18. Singhvi, M. S., Zinjarde, S. S., & Gokhale, D. V. (2019). Polylactic acid: Synthesis and biomedical applications. Journal of Applied Microbiology, 127(6), 1612–1626.
19. Torrado Perez, A. R., Roberson, D. A., & Wicker, R. B. (2015). Fracture surface analysis of 3D-printed tensile specimens of novel ABS-based materials. Journal of Failure Analysis and Prevention, 15(1), 154–164.

20. Ning, F., Cong, W., Qiu, J., Wei, J., & Wang, S. (2015). Additive manufacturing of carbon fiber reinforced thermoplastic composites using fused deposition modeling. Composites Part B: Engineering, 80, 369–378
21. Chung, D. D. L. (2012). Carbon fiber composites. Butterworth-Heinemann.
22. Tekinalp, H. L., Kunc, V., Velez-Garcia, G. M., Duty, C. E., Love, L. J., Naskar, A. K., Blue, C. A., & Ozcan, S. (2014). Highly oriented carbon fiber–polymer composites via additive manufacturing. Composites Science and Technology, 105, 144–150.
23. Love, L. J., Kunc, V., Rios, O., Duty, C. E., Elliott, A. M., Post, B. K., Smith, R. J., & Blue, C. A. (2014). The importance of carbon fiber to polymer additive manufacturing. Journal of Materials Research, 29(17), 1893–1898.
24. Lanzotti, A., Grasso, M., Staiano, G., & Martorelli, M. (2015). The impact of process parameters on mechanical properties of parts fabricated in PLA with an open-source 3D printer. Rapid Prototyping Journal, 21(5), 604–617.
25. Boschetto, A., & Bottini, L. (2014). Accuracy prediction in fused deposition modeling. The International Journal of Advanced Manufacturing Technology, 73(5–8), 913–928.
26. Álvarez, K., Lagos, R. F., & Aizpun, M. (2016). Investigating the influence of infill percentage on mechanical properties of fused deposition modelled parts. Ingeniare. Revista Chilena de Ingeniería, 24(1), 17–24.
27. Coogan, T. J., & Kazmer, D. O. (2017). Bond and part strength in fused deposition modeling. Rapid Prototyping Journal, 23(2), 414–422.
28. Dawoud, M., Taha, I., & Ebeid, S. J. (2016). Mechanical behaviour of ABS: An experimental study using FDM and injection moulding techniques. Journal of Manufacturing Processes, 21, 39–45.
29. Farah, S., Anderson, D. G., & Langer, R. (2016). Physical and mechanical properties of PLA, and their functions in widespread applications — A comprehensive review. Advanced Drug Delivery Reviews, 107, 367–392.

30. Seppala, J. E., & Migler, K. D. (2016). Infrared thermography of welding zones produced by polymer extrusion additive manufacturing. Additive Manufacturing, 12, 71–76.
31. Sood, A. K., Ohdar, R. K., & Mahapatra, S. S. (2010). Parametric appraisal of mechanical property of fused deposition modelling processed parts. Materials & Design, 31(1), 287–295.
32. Bhandari, S., Lopez-Anido, R. A., & Gardner, D. J. (2019). Enhancing interlayer tensile strength of 3D printed short carbon fiber reinforced PLA composites. Composites Part B: Engineering, 172, 54–65.
33. Rankouhi, B., Javadpour, S., Delfanian, F., & Letcher, T. (2016). Failure analysis and mechanical characterization of 3D printed ABS with respect to layer thickness and orientation. Journal of Failure Analysis and Prevention, 16(3), 467–481.
34. Lee, C. S., Kim, S. G., Kim, H. J., & Ahn, S. H. (2007). Measurement of anisotropic compressive strength of rapid prototyping parts. Journal of Materials Processing Technology, 187–188, 627–630.
35. Rodriguez, J. F., Thomas, J. P., & Renaud, J. E. (2003). Mechanical behavior of acrylonitrile butadiene styrene fused deposition materials modeling. Rapid Prototyping Journal, 9(4), 219–230.
36. Es-Said, O. S., Foyos, J., Noorani, R., Mendelson, M., Marloth, R., & Pregger, B. A. (2000). Effect of layer orientation on mechanical properties of rapid prototyped samples. Materials and Manufacturing Processes, 15(1), 107–122.
37. Yunus, M., & Alsoufi, M. S. (2020). Effect of raster inclinations and part positions on mechanical properties, surface roughness and manufacturing price of printed parts produced by fused deposition method. *Journal of Mechanical Engineering and Sciences*, *14*(4), 7416-7423

38. Gao, G., Xu, F., Xu, J., Tang, G., & Liu, Z. (2022). A survey of the influence of process parameters on mechanical properties of fused deposition modeling parts. *Micromachines*, *13*(4), 553.
39. Dey, A., & Yodo, N. (2019). A systematic survey of FDM process parameter optimization and their influence on part characteristics. *Journal of Manufacturing and Materials Processing*, *3*(3), 64.
40. Jabeur, M., & Souissi, S. (2026). Optimization of Process Parameters and Materials Selection in FDM: A Review. *Journal of Applied Polymer Science*, *143*(21), e70695.
41. Narang, R., & Chhabra, D. (2017). Analysis of process parameters of fused deposition modeling (FDM) technique. *International Journal on Future Revolution in Computer Science & Communication Engineering*, *3*(10), 41-48.
42. Datta, S., Bandyopadhyay, A., & Pal, P. K. (2009). Grey-based Taguchi method for optimization of bead geometry in submerged arc bead-on-plate welding. *The International Journal of Advanced Manufacturing Technology, 39*(11–12), 1136–1143.
43. Srinivasan, R., Ruban, W., Deepanraj, B., Bhuvanesh, R., & Bhuvanesh, T. (2020). Effect on infill density on mechanical properties of PETG part fabricated by fused deposition modelling. Materials Today: Proceedings, 27, 1838–1842.
44. ASTM International. (2014). ASTM D638-14: Standard test method for tensile properties of plastics. ASTM International.
45. Wang, P., Zou, B., Xiao, H., Ding, S., & Huang, C. (2021). Effects of printing parameters of fused deposition modeling on mechanical properties, surface quality, and microstructure of PLA composites. Polymers, 13(3), 1–18.
46. Zhang, X., Chen, L., Mulholland, T., & Osswald, T. A. (2019). Effects of raster angle on the mechanical properties of PLA and Al/PLA composite part produced by fused deposition modeling. *Polymers for Advanced Technologies*, *30*(8), 2122-2135.

47. Liu, X., Zhang, M., Li, S., Si, L., Peng, J., & Hu, Y. (2017). Mechanical property parametric appraisal of fused deposition modeling parts based on the gray Taguchi method. *The International Journal of Advanced Manufacturing Technology*, *89*(5), 2387-2397.
48. Tymrak, B. M., Kreiger, M., & Pearce, J. M. (2014). Mechanical properties of components fabricated with open-source 3-D printers under realistic environmental conditions. *Materials & Design*, *58*, 242-246.
49. Xinhua, L., Shengpeng, L., Zhou, L., Xianhua, Z., Xiaohu, C., & Zhongbin, W. (2015). An investigation on distortion of PLA thin-plate part in the FDM process. *The International Journal of Advanced Manufacturing Technology, 79(5), 1117-1126.*
50. Chung Wang, C., Lin, T. W., & Hu, S. S. (2007). Optimizing the rapid prototyping process by integrating the Taguchi method with the Gray relational analysis. *Rapid prototyping journal*, *13*(5), 304-315.
51. Aslani, K. E., Chaidas, D., Kechagias, J., Kyratsis, P., & Salonitis, K. (2020). Quality performance evaluation of thin walled PLA 3D printed parts using the taguchi method and grey relational analysis. *Journal of Manufacturing and Materials Processing*, *4*(2), 47.
52. Tunçel, O., Tüfekci, K., & Kahya, Ç. (2024). Multi-objective optimization of 3D printing process parameters using gray-based Taguchi for composite PLA parts. *Polymer Composites*, *45*(14), 12870-12884.
53. Arockiam, A. J., Rajesh, S., Karthikeyan, S., & Sathishkumar, G. B. (2024). Optimization of fused deposition 3D printing parameters using taguchi methodology to maximize the strength performance of fish scale powder reinforced PLA filaments. International Journal on Interactive Design and Manufacturing (IJIDeM), 18(6), 3813-3826.
54. Tunçel, O. (2024). Optimization of Charpy impact strength of tough PLA samples produced by 3D printing using the Taguchi method. Polymers, 16(4), 459.

55. Kilinc, F. B., Turkoglu, T., Guler, S., & Kilinc, A. C. (2025). Optimization of 3D printing parameters for enhanced tensile properties in continuous carbon fiber reinforced PLA composites. Materials Research Express, 12(4), 045302.
56. Ning, F., Cong, W., Hu, Y., & Wang, H. (2017). Additive manufacturing of carbon fiber-reinforced plastic composites using fused deposition modeling: Effects of process parameters on tensile properties. Journal of composite materials, 51(4), 451-462.
57. Kamaal, M., Anas, M., Rastogi, H., Bhardwaj, N., & Rahaman, A. (2021). Effect of FDM process parameters on mechanical properties of 3D-printed carbon fibre–PLA composite. Progress in Additive Manufacturing, 6(1), 63-69.
58. Reverte, J. M., Caminero, M. Á., Chacón, J. M., García-Plaza, E., Núñez, P. J., & Becar, J. P. (2020). Mechanical and geometric performance of PLA-based polymer composites processed by the fused filament fabrication additive manufacturing technique. Materials, 13(8), 1924.
59. Kargar, E., & Ghasemi-Ghalebahman, A. (2023). Experimental investigation on fatigue life and tensile strength of carbon fiber-reinforced PLA composites based on fused deposition modeling. Scientific Reports, 13(1), 18194.
60. Kumar, K. R., Mohanavel, V., & Kiran, K. (2022). Mechanical properties and characterization of polylactic acid/carbon fiber composite fabricated by fused deposition modeling. Journal of materials engineering and Performance, 31(6), 4877-4886.
61. Tang, C., Liu, J., Yang, Y. A. N. G., Liu, Y., Jiang, S., & Hao, W. (2020). Effect of process parameters on mechanical properties of 3D printed PLA lattice structures. Composites Part C: Open Access, 3, 100076.
62. Fraj, B. B., & Ahmed, Z. (2025). Thermal, structural, and mechanical properties of carbon fiber reinforced PLA composites: influence of FDM print speed and comprehensive analysis. Polymer Composites, 46(18), 17229-17239.

63. Mishra, V., Bharat, N., Kumar, V., Vellaisamy, M., & Veeman, D. (2025). Multi-objective optimization of 3D printed PLA/carbon fibre composite using a combined approach of gray relational analysis and ANOVA. Journal of Thermoplastic Composite Materials, 38(11), 4208-4227.
64. Abdallah S, Ali S, Pervaiz S. Performance optimization of 3D printed polyamide 12 via multi jet fusion: a Taguchi grey relational analysis (TGRA). *Int J Light Mater Manuf*. 2023; **6**: 72-81.
65. Arifin F, Zamheri A, Herlambang YD, Syahputra AP, Apriansyah I, Franando F. Optimization of process parameters in 3D printing Fdm by using the Taguchi and Grey relational analysis methods. *SINTEK J J Ilm Tek Mesin*. 2021; **15**: 1.
66. Patil, P., Singh, D., Raykar, S. J., & Bhamu, J. (2021). Multi-objective optimization of process parameters of Fused Deposition Modeling (FDM) for printing Polylactic Acid (PLA) polymer components. Materials Today: Proceedings, 45, 4880-4885.
67. Rasheed, A., Hussain, M., Ullah, S., Ahmad, Z., Kakakhail, H., Riaz, A. A., ... & Khan, I. (2023). Experimental investigation and Taguchi optimization of FDM process parameters for the enhancement of tensile properties of Bi-layered printed PLA-ABS. Materials Research Express, 10(9), 095307.
68. Mustafa, M. S., Zafar, M. Q., Muneer, M. A., Arif, M., Siddiqui, F. A., & Javed, H. M. A. (2020). Process parameter optimization in fused deposition modeling (FDM) using response surface methodology (RSM). Res. Sq, 19.
69. Singh, M., & Bharti, P. S. (2022). Grey relational analysis-based optimization of process parameters for efficient performance of fused deposition modelling based 3D printer. J Eng Res, 10(2021), 1-15.
70. Bochnia, J., Blasiak, M., & Kozior, T. (2021). A comparative study of the mechanical properties of FDM 3D prints made of PLA and carbon fiber-reinforced PLA for thin-walled applications. *Materials*, *14*(22), 7062

71. Caminero, M. A., Chacón, J. M., García-Moreno, I., & Reverte, J. M. (2018). Interlaminar bonding performance of 3D printed continuous fibre reinforced thermoplastic composites using fused deposition modelling. *Polymer Testing*, *68*, 415-423

72. Fraj, B. B., & Ahmed, Z. (2025). Thermal, structural, and mechanical properties of carbon fiber reinforced PLA composites: influence of FDM print speed and comprehensive analysis. *Polymer Composites*, *46*(18), 17229-17239

73. Ayatollahi, M. R., Nabavi-Kivi, A., Bahrami, B., Yahya, M. Y., & Khosravani, M. R. (2020). The influence of in-plane raster angle on tensile and fracture strengths of 3D-printed PLA specimens. *Engineering Fracture Mechanics*, *237*, 107225

74. Vălean, E., Marşavina, L., Galaţanu, S. V., Foti, P., & Berto, F. (2025). Are carbon fibres beneficial to improve mechanical and fracture properties of FDM printed composites?. *Engineering Fracture Mechanics*, 111791.

75. Chandrasekaran, N. K., & Subramani, V. (2026). Flexural performance and failure behavior of additively manufactured continuous carbon fiber-reinforced polylactic acid composites. *Journal of Materials Research*, *41*(9), 1391-1407.